Carnegie Observatories Astrophysics Series, Vol. 3:
Clusters of Galaxies: Probes of Cosmological Structure and Galaxy Evolution
ed. J. S. Mulchaey, A. Dressler, and A. Oemler (Pasadena; Carnegie Observatories:
http://www.ociw.edu/ociw/symposia/series/symposium3/proceedings.html)

Diffuse Optical Light in A3888

J. KRICK & R. BERNSTEIN
The University of Michigan

Abstract

Surface brightness measurements of the diffuse intracluster light(ICL) in centrally concentrated, relaxed clusters have demonstrated that stars bound only to the cluster potential can contain anywhere from 5-50% of the total cluster flux. As such, this intracluster component is a considerable fraction of the stellar population and can be used to constrain models for the structure and evolution of clusters and their member galaxies. We are undertaking a program to measure the characteristics of the ICL (total flux, color, and substructure) as a function of cluster mass, morphology, and redshift. Our sample includes clusters at low and moderate redshifts, observed with the LCO 40 inch telescope (B- and r-band) and 100 inch telescope (V- and r-band) respectively. We present here the preliminary reductions and analysis of one cluster in that sample, A3888. With 4-5 hour integration times on-source per filter, we have obtained sensitivities of ~ 30.3 mag arcsec $^{-2}$ in gunnr band over arcminute scales and ~ 29.5 mag arcsec $^{-2}$ at the spatial resolution of the data.

1.1 Introduction

The diffuse ICL is a population of stars not bound to any galaxy in the cluster, but to the cluster potential itself. Studying the ICL can give insight into the processes influencing galaxy formation and evolution in clusters. These processes include interactions among galaxies, interactions between galaxies and the cluster potential, and ram pressure stripping. Measurements of the color, total flux, structure, and redshift dependence will help to differentiate between these models and their relative influence on the evolution of galaxies in clusters

Previous studies have found that 5-50% of the total light in clusters comes from the intracluster stars (see Feldmeier et al. 2002 and references therein). Low surface brightness measurements of the diffuse ICL are complemented by searches for the individual stars in the nearest clusters in the form of red giants, planetary nebulae, and supernovae.

1.2 The Program

We are beginning a program to measure the ICL component in ten galaxy clusters which requires measuring a signal that is $\sim 1\%$ of the sky level. We intend to constrain total flux, color, and morphology of the ICL as a function of cluster mass, morphology, and redshift. Color information will be used to deduce the parent population of these stars. Our data also contain the more obvious results of galaxy interactions; namely tidal features.

The sample includes ten clusters which were first and foremost selected to be at high

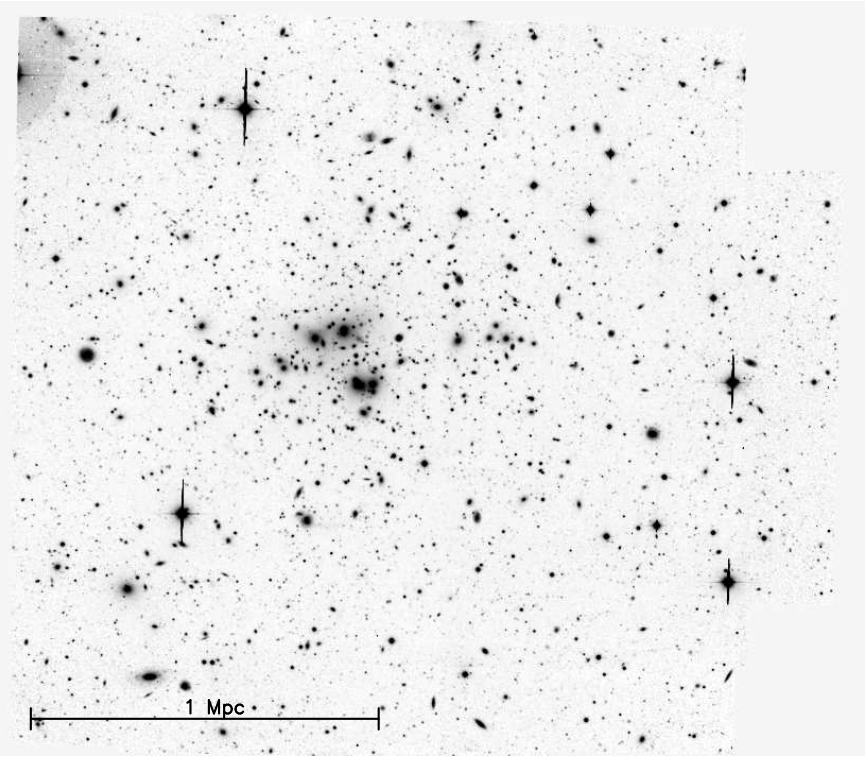

Fig. 1.1. The combined, background–subtracted V–band image of A3888 from our LCO 100–inch observations. The gray–scale is linear over the range 25–29.5 mag arcsec^{-2}.

galactic latitude, thereby reducing possible complications from bright stars and galactic foregrounds. The clusters were chosen to have published X-ray luminosities as well as redshift measurements for a reasonable fraction of member galaxies. Table 1 shows the characteristics of the clusters in the sample. Bautz/Morgan types range from I to III where type I clusters have cD galaxies and type III clusters do not. Richness class is defined by Abell as a scale ranging from 0 to 5, with 5 being the richest clusters.

1.3 Status and Preliminary Results

Data for all ten clusters is in hand. The low redshift population was imaged in 900 second B and gunnr exposures with the Las Campanas Swope 40" telescope. The mid-distance population was imaged in V and gunnr with the duPont 100" telescope. A3888 was chosen as the first cluster to be processed due to high quality observing conditions and a wealth of information on this cluster in the literature.

Standard reductions were performed on the cluster images. Night sky flats were used for large scale flat-fielding which is accurate to better than 0.05% of the sky level. To insure that background sky removal is not a significant source of error, we employed a dithering program at the telescope to maximize time on-source as well as capturing off-source background sky levels in each frame. As contamination from bright stars is a concern, we have

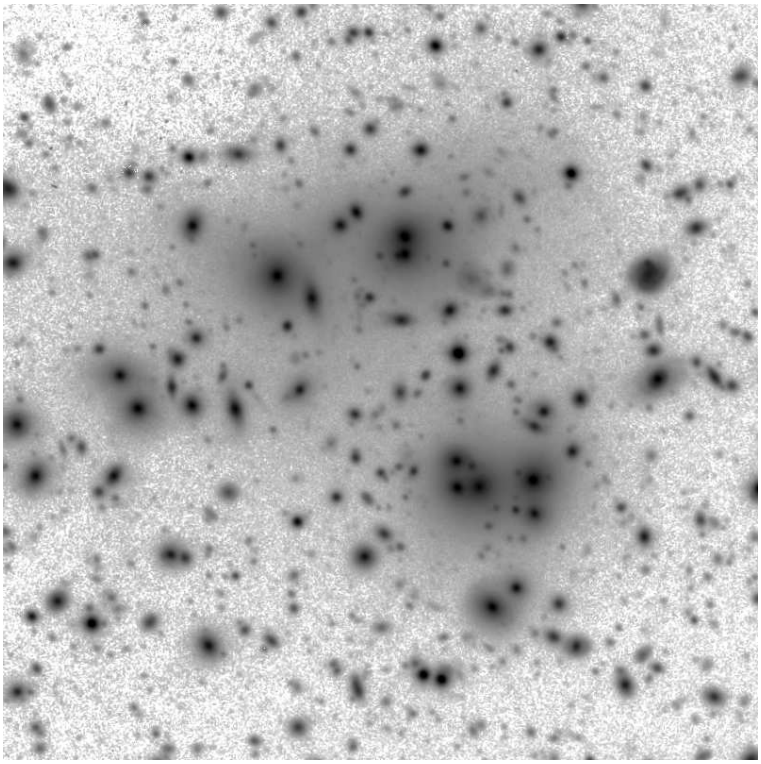

Fig. 1.2. The center of A3888 in V (see Figure 1). The gray–scale is linear over the range 20.4–29.5 mag arcsec^{-2}.

mapped the point spread function (psf) out to $\sim$ 10 arcminutes at multiple positions around the CCD using bright stars. At the present stage in processing we are able to measure large scale surface brightness features at $\sim$ 30.3 r mag arcsec $^{-2}$ and $\sim$ 29.5 r mag arcsec^{-2} at the resolution of the images.

Figure 1 shows a combined 4.3 hour V-band exposure of the entire field of A3888. Zooming in to the center of this image shows evidence of a diffuse component in the cluster core (figure 2). Preliminary investigation reveals interesting low surface brightness features in our combined image (figure 3). Low surface brightness features will be easier to distinguish after the galaxies are modeled and subtracted from the images.

References

Abell, G.O., Corwin, H.G., Jr., & Olowin, R.P. 1989, ApJS, 70, 1
Busarello, G., Merluzzi, P., La Barbera, F., Massarotti, M., & Capaccioli, M. 2002, AA, 389, 787
Chen, J., Huchra, J.P., McNamara, B.R., & Mader, J. 1998, AAS, 193, 3912
Ciardullo, R., Ford, H.,& Harms, R. 1985, ApJ, 293, 69
Collins, C.A.; Guzzo, L.; Nichol, R.C.; & Lumsden, S.L. 1995, MNRAS, 274, 1071
Couch, W.J. & Newell, E.B. 1984, ApJS, 56, 143
Couch, W.J. & Sharples, R.M. 1987, MNRAS, 229, 423
Couch, W.J., Balogh, M.L., Bower, R.G., Smail, I., Glazebrook, K., & Taylor, M. 2001, ApJ, 549, 820
den Hartog, R. 1995, Ph.D. Thesis, Univ. Leiden
De Propris et.al. 2002, preprint (astro-ph/0212562)

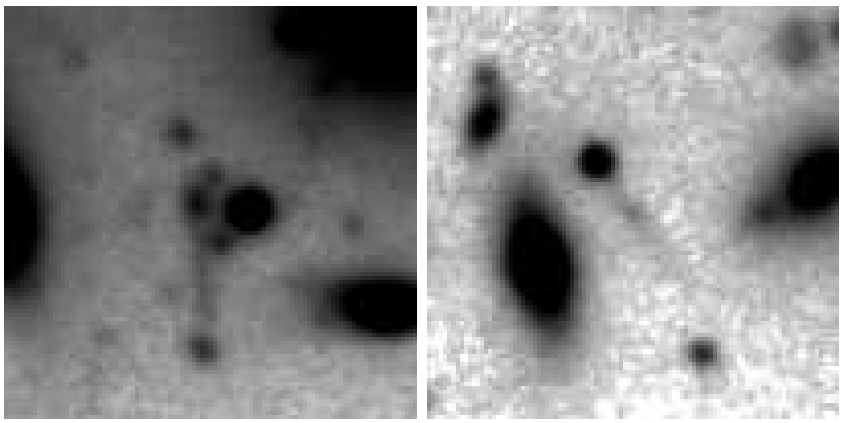

Fig. 1.3. Two low surface brightness feature from the $V-$band image (Figure 3). The images are plotted with a gray–scale range of 23.7–27.2 mag arcsec^{-2}. In the image on the left, a feature which appears to be tidal debris (tails extending up and down) is visible to the left of the compact galaxy near the center. In the image on the right, a very low surface brightness feature extends to the lower right hand corner from the compact galaxy above and left of the center. The nature of both features may be easier to interpret after we have modeled and subtracted the brighter resolved galaxies.

Ebeling, H., Voges, W., Bohringer, H., Edge, A.C., Huchra, J.P., & Briel, U.G. 1996, MNRAS, 281, 799
Fadda, D., Girardi, M., Giuricin, G., Mardirossian, F., & Mezzetti, M. 1996, ApJ, 473, 670
Feldmeier, J.J., Mihos, J. C., Morrison, H.L., Rodney, S.A., & Harding, P. 2002, ApJ, 575, 779
Girardi, M.; Borgani, S.; Giuricin, G.; Mardirossian, F.; & Mezzetti, M. 1998, ApJ, 506, 45
Girardi, M. & Mezzetti, M. 2001, ApJ, 548, 79
Kowalski, M.P., Ulmer, M.P., & Cruddace, R.G. 1983, ApJ, 268, 540
Moore, B., Katz, N., Lake, G., Dressler, A., & Oemler, A., Jr. 1996, Nature, 379, 613
Moore, B., Lake, G., & Katz, N. 1998, ApJ, 495, 139
Mazure, A., et al. 1996, AA, 310, 31
Peacock, J.A. & West, M.J. 1992, MNRAS, 259, 494
Stein, P. 1997, ‘ AA, 317, 670
Struble, M.F.& Rood, H.J. 1999, ApJS, 125, 35
Teague, P.F.; Carter, D.; & Gray, P.M. 1990, ApJS, 72, 715
Wu, X. P.; Xue, Y. J.; & Fang, L. Z. 1999, ApJ, 524, 22

Table 1.1Cluster Characteristics

cluster name	ra (J2000) (hr:mm)	dec (J2000) (dd:mm)	l (degrees)	b (degrees)	z	B/M	Richness Class	L_x (0.1–2.4 keV) 10^{44}ergs/s[a]	σ_v km/s	Number of measured redshifts	n(HI)[a] 10^{20}cm^{-2}	lensing measurement
A4059	23:57	-34:40	356.8	-76.06	0.048[b]	I	1	3.09	845^{+280}_{-140}[u]	45[g,j]	1.1	—
A3880	22:28	-30:34	17.99	-58.50	0.058[b]	II	0	1.86	827^{+120}_{-79}[v]	122[h,o,d]	1.1	—
A2734	00:11	-28:52	19.46	-80.98	0.062[b]	III	1	2.55	628^{+61}_{-57}[v]	127[i,j,k,d]	1.8	—
A2556	23:13	-21:38	41.37	-66.97	0.087[b]	II-III	1	2.47	1247^{+249}_{-249}[u]	2[l,m]	2.0	—
A4010	23:31	-36:30	359.0	-70.60	0.096[b]	I-II	1	5.55	625^{+127}_{-95}[v]	30[i,j]	1.4	—
A3888	22:34	-37:43	3.96	-59.40	0.151[b]	I-II	2	14.52	1102^{+137}_{-107}[w]	98[n]	1.2	—
A3984	23:15	-37:48	359.0	-67.19	0.181[b]	II-III	2	9.18	—	12[j,o]	1.7	—
A0141	01:06	-24:35	175.3	-85.93	0.23[b]	III	3	12.62	—	0 [c]	1.8	Dahle et al. (2002)
AC118	00:14	-30:2	8.90	-81.24	0.308[b]	III	3	22.05	1947^{+292}_{-201}[r]	489[e,p,q,r]	1.7	Smail et al. (1991)
AC114	22:58	-34:47	8.32	-64.78	0.31[c]	II-III	2	7.0	1388^{+128}_{-71}[w]	103[f,r]	2.0	Smail et al. (1991)

Notes: a: Ebeling et al. (1996). b: Struble & Rood (1999). c: Abell, Corwin, & Olowin (1989). d: De Propris et al. (2002). e: Busarello et al. (2002) f: Couch et al (2001). g: Chen et al (1998). h: Stein (1997). i: den Hartog (1995). j: Mazure et al. (1996). k: Fadda et al. (1996). l: Ciardullo, Ford, & Harms, (1985). m: Kowalski, Ulmer, & Cruddace, (1983). n: Teague, Carter, & Gray, (1990). o: Collins et al. (1995). p: Peacock & West (1992). q: Couch & Newell (1984). r: Couch & Sharpless (1987). u: Wu, Xue, & Fang (1999). v: Girardi et al. (1998). w: Girardi & Mezetti (2001).